Advances in Nonlinear Variational Inequalities
ISSN: 1092-910X
Vol 27 No. 2 (2024)

A Novel Perspective on the Quality Index for Fused Satellite Images

Milind S. Patil[1,2], Pradeep B Mane[3]

[1] Research Scholar, AISSMSIoIT, Pune
[2] Assistant Professor VIIT, Pune
[3] Principal, AISSMSIoIT, Pune

[1]milind.patil@viit.ac.in

[3]pbmane6829@gmail.com

Article History:

***Received**: 05-02-2024*

***Revised**: 20-04-2024*

***Accepted**: 10-05-2024*

Abstract:

Blind Image Quality Assessment for Remote Sensing Applications has garnered a significant amount of interest from the community, presenting a problem that is both persistent and difficult to solve. The current quality indicators are, for the most part, in agreement with each individual's subjective perception. Traditional handcrafted quality measures focus on detecting low-level features such as contour, edge, color, texture, and shape. These are the attributes that will be measured. Nevertheless, it is possible that they will disregard the essential semantics that lie behind the warped image. Within the scope of popular deep learning, the process of acquiring multilayer features is a straightforward exercise. The unfortunate reality is that a significant number of these models either ignore superficial traits or focus only on high-level variables, which ultimately leads to poor prediction performance. In order to successfully portray varying degrees of distortion, the fusion features make advantage of the laws that govern the human visual system in order to extract both local and global components of information. In conclusion, the ultimate quality score is determined by considering the features of both the local and global levels. In this investigation, we developed two different NR-IQA methods. In one, a markov random field is used, while in the other, a sparse approximation variational autoencoder is established as the foundation. The effectiveness of our work is shown by the evaluation of multiple IQA datasets, where our model consistently generates findings that are at the leading edge of the field. This evaluation does not make use of any quality standards; rather, it compares it against a variety of well-known cutting-edge techniques and average opinion ratings based on the opinions of different people. Quality ratings are accurately predicted by the regression models that have been provided.

Keywords: Deep neural networks (DNNs) Sparse approximation variational autoencoder. Quality evaluation Regression Model: no-reference image quality evaluation, level set, Markov random field, fuzzy clustering, NR-IQA.

1. Introduction

It is essential to evaluate the quality of satellite pictures in order to determine whether or

not the equipment used to gather satellite photos is operating correctly and to design algorithms for image processing. It has a direct impact on the degree of accuracy with which information is collected from remote sensing [1]. The NR-IQA approach, which is often referred to as the BIQA technique, is a method that may automatically evaluate the quality of a photograph without the requirement for a pristine version to be compared from [2]. IQA encompasses both subjective and objective forms of evaluation [3]. Objective IQAs have become more popular as deep learning algorithms have evolved. This is due to the fact that they provide an alternative to subjective IQA that is both more efficient and requires less input from the user. IQA, also known as objective blind or no-reference (NR) image quality assessment, is a method of evaluating picture quality that is carried out via the use of an algorithm. No prior information is gathered by the algorithm before it begins to make a prediction about the quality of the distorted image. Assessing the quality of an image without any reference or guidance is a task that is very difficult to do. The ability to accurately predict quality has been shown by systems that are based on comparing photographs to a reference. Researchers often approach the problem of NR IQA by breaking it down into a series of smaller problems that are relevant to a certain area. They focus on a limited number of artefacts and distortion-specific identification and quality assurance. As the accuracy of picture quality prediction has increased, particularly via the use of deep learning-based algorithms, traditional no-reference image quality assessment (NR-IQA) procedures have undergone significant advancements. In spite of this, the free-energy principle-guided NR-IQA processes that are used by this approach are not successful in efficiently restoring badly damaged photographs. One of the consequences of this is that it is impossible to exactly evaluate the quality reconstruction relationship between the image that has been damaged and the picture that has been restored. At this time, there is not a single NR-IQA algorithm that has shown a consistent connection with human evaluations of subjective temporal visual quality. In the event that deviations from natural statistics are accurately measured, it is possible to develop algorithms that can assess the perceptual quality of a picture without relying on a reference image. The purpose of this study was to offer an NR-IQA technique that relies just on basic image visual criteria for learning, hence removing the need for human-scored picture libraries. Through our demonstration, we established that these components are essential for shaping an image and influencing the visual appeal of the picture. We introduced the Visual Evaluation Index (VEI), which is a tool for evaluating pictures that does not rely on references and instead employs visual measurements to evaluate image quality.

The following is the structural arrangement of the remaining parts of the paper: In the second section, a review of the most recent quality assessment techniques follows, followed by a discussion of the primary drawbacks of the ones that are now in use. Section 3 contains a discussion of the model that was proposed. Within the fourth section of the study, the analysis of the experiment that was utilized to evaluate performance metrics is presented. Last but not least, some closing reflections are included in Section 5.

2. Literature Survey:

In the beginning of the study on no reference quality assessment, models were developed to

correct picture faults such as blurriness, graininess, blockiness, and ringing. This was the beginning of the assessment. Blurring, noise, or compression artefacts were the root causes of these technical difficulties. Participants ranged in age from 18 to 21 years old. Throughout the course of their research, L.Hu et al.[4] provide a novel BIQA approach that places equal focus on both synthetic and actual distortion. They present a framework for a visual transformor that is configurable and utilizes hierarchical feature fusion in order to improve the accuracy of the evaluation. An effective vision-Transformer backbone is used in the first portion of the approach, which is the extraction of multiscale features. In addition, a hierarchical feature fusion module is provided so that features from various levels may be progressively integrated into the system. The elimination of redundant information is accomplished in a straightforward and efficient way by using an attention mechanism that is implemented immediately after each fusion. In their research work, S. Bosse and colleagues [5] proposed a method for evaluating picture quality, which they referred to as the image quality assessment (IQA). As part of this approach, a deep neural network is used. Ten convolutional layers and five pooling layers constitute the network, which is trained from the very beginning to the very end. The pooling layers are used for feature extraction. In addition to this, it has two regression layers that are completely interconnected, which makes it a great deal more thorough than prior IQA models. In their research, W. Zhang and his colleagues [6] constructed a deep bilinear model that is capable of accurately rating the quality of a photograph, regardless of whether the photos were altered purposefully or organically. For the purpose of providing a final quality forecast, the two feature sets are blended into a single representation. Following that, a modified form of stochastic gradient descent should be used in order to optimize the whole network on the databases that are being taking into account. During the course of their research, J. Wu and his colleagues [7] presented a CNN method for blind IQA (BIQA). This technique is capable of accurately taking into account the quality drop. Despite the fact that CNN is highly dependent on enormous volumes of data, the IQA databases that are now available are not sufficient to meet the requirements necessary to optimize its operations. Additionally, W. Zhang and his colleagues [8] developed a unified BIQA model as well as a training technique that is capable of dealing with both synthetic and true aberrations. For the purpose of improving the performance of a deep neural network for BIQA, they compare an extremely large number of picture couplings. Integrity loss is the method that is used to accomplish this. In addition, they suggest the use of a hinge constraint in order to guarantee a more precise assessment of uncertainty throughout the process of optimization.

The ranking is based on a controllable list. IQA, also known as CLRIQA, is an innovative rank learning-based NR-IQA technique that was published by OU et al. [9]. Using the inverse of the Weber-Fechner rule, this method assesses whether or not there is an excessive or insufficient exposure. Fusion and compression techniques are used in order to create rank picture samples and imitate the effects of real-world distortion. Two distinct components make up the VCRNet, which was created by Pan Z and his colleagues [10]. These components include a quality rating network and a visual restoration network. The purpose of this is to establish a connection that is suitable between the distorted and restored images. A visual compensation module, an optimized asymmetric residual block, and an error map-based mixed

loss function are the components that make up the network model. Liu C. and colleagues [11] provide a multi-level feature augmentation technique that may be used to retrieve local features from photographs that have been previously distorted. The above paragraph provides an illustration of this tactic. Deep pan sharpening was the subject of a quality assurance network that was constructed by N. Badal and colleagues [12]. To do this, it establishes the equivalence of feature representations that are derived from panchromatic and input low resolution multispectral photos that have properties that are comparable to one another. The self-supervised collaborative autoencoder that Z. Zhou and colleagues [13] have developed is shown here. Additionally, this autoencoder is able to differentiate between distortion and information that is connected to the content material. In addition to this, they provide a quality predictor that is based on self-adaptive weighting, which guarantees that the content and distortions are suitably balanced when estimating the quality of the image. Yang et al. [14] developed a saliency-guided architecture that includes spatial and transposed attention. This architecture is based on NR-IQA and operates from beginning to finish.

Here are some commonly used NR-IQA methods:

i. BRISQUE (Blind/Reference less Image Spatial Quality Evaluation) uses spatial attributes to evaluate quality [2-22].
ii. PIQE (Perceptual Image Quality Estimate) is a quality assessment approach that uses spatial information, like BRISQUE [24-25].
iii. The NIQE (Natural Image Quality Evaluator) assesses spatial and frequency domain characteristics [26].

3. Methodology:

The quantity of distortions or noise that a picture contains is the same thing that is considered while assessing the quality of the image. Obtaining accurate evaluations of these quality indicators is challenging due to the absence of a reference image. The method that is referred to as general-purpose no-reference image quality assessment (NR-IQA) was first developed with the intention of evaluating the quality of the picture without taking into consideration the various kinds of distortion [15] - [16]. The approach that is being used here is to make use of extracted qualities that have the potential to aid in detecting various types of distortion. As a consequence of this, the performance of the product is directly proportional to the architecture of its many components. However, the most basic problems with the satellite image datasets that are now available are that 1) they have a limited range of content and distortions, and 2) they do not accurately represent complex combinations of distortions that are frequent in photos captured in the real world. Both of these problems plague the satellite image datasets. In addition, there is no reference image that can be accessed, and it is not apparent how the human visual system (HVS) distinguishes between the various levels of picture quality and authenticity.

A) Sparse Approximated Variational Autoencoder (SAVA) IQA:

Alternative autoencoders, also known as variational autoencoders or VAEs, are models that address a specific challenge that is associated with conventional autoencoders. A condensed

form of the input, also known as the latent space or bottleneck, is the sole form that an autoencoder learns to represent throughout the course of its training. On the other hand, the latent space that is formed as a result of training is not necessarily continuous and in certain cases may be difficult to interpolate. This is the specific difficulty that variational autoencoders [27], which describe the latent properties of the data as a probability distribution, are designed to answer. In this way, a continuous latent space is produced, which may be sampled and interpolated with relative ease. An strategy that is often used for learning sparse codes involves repeatedly applying the recursive equation that is shown below until convergence is reached. In order to solve the problem of l1-norm regularized least squares in sparse codebooks, the authors of this work suggest the use of an iterative sparse approximation that is accompanied by a pre-conditioner that is unique to itself.

In order to produce sparse code $x \in \mathbb{R}^{\eta}$ from noisy input, this method is used. The following is an example of a general sparse approximation:

$$\mathfrak{b} = \mathcal{A}x + n \in \mathbb{R}^{\mathrm{M}} \qquad (1)$$

Where $\mathcal{A} \in \mathbb{R}^{\mathrm{MxN}}$and $n \in \mathbb{R}^{\mathrm{M}}$ is the environmental noise.

A huge amount of data points are needed for the conventional Least Squares (LS) method.

$\mathcal{M} \geq \mathcal{N}$and $\mathcal{A}$ has full rank $\mathcal{N}$ to recover $\dot{x} = (\mathcal{A}^{\mathcal{T}}\mathcal{A})^{-1}\mathcal{A}^{\mathcal{T}}\mathfrak{b}$. A much lower number of observations, $\mathcal{M} \leq \mathcal{N}$ might be used to reconstruct x using current Compressed Sensing (CS) methods. The previously noted challenge with basis-based image content representation may be overcome so long as the input picture seems sparse:

$$\min_{xe\mathbb{R}^N} \frac{1}{2}\|Ax - b\|^2 + \tau\|x\|_1 \qquad (2)$$

Where $\tau > 0$ is a specified normalization coefficient, $\|x\| = \sqrt{\sum_{i=1}^{N} x_i^2}$ and $\|x\|_1 = \sqrt{\sum_{i=1}^{N}|x_i|}$denote the$l_2$and the $l_1$norms of x, respectively,

Incorporating the restriction clarifies the solution key space. The data would be extracted utilizing an effective optimization method in the suggested recovery procedure.

$\hat{x} = [x^+; x^-] \in \mathbb{R}^{2N} \geq 0and\hat{A} = [A, -A] \in \mathbb{R}^{M_x 2N}$(3)

where, $x_i^+ = \max(x_i, 0)$ and $x_i^- = \max(-x_i, 0)$, the $Ax = \hat{A}\hat{x}$ and, $\|x\|_{1=}\|\hat{x}\|_1$and hence Eq.) can be solved with respect to $\hat{A}$ and. $\hat{x} \geq 0$.

Thus, the proposed method need just identify the form of Eq. shown below.

for $x \geq 0$

$$\min_{xe\mathbb{R}^N} \frac{1}{2}\|Ax - b\|^2 + \tau e^{\tau}x(4)$$

$$stx \geq 0$$

An optimized solution may be found using the Karush-Kuhn-Tucker (KKT) system if the optimization problem in Equation (4) is convex and contains only linear constraints that satisfy Slater's condition:

$$A^{\tau}Ax - s - A^{\tau}b + \tau e = 0 \qquad (5a)$$

$$X.Se = 0 \qquad (5b)$$

$$(x, s) \geq 0 \qquad (5c)$$

Where

$$X = Diag(x) and S = Diag(s)$$

from implication, diagonal matrices are composed of the primal coefficient x and the dual coefficient values x and s, respectively. This is implied from the equation that was shown before. In addition, it was observed that the values 0 and e represent arrays that are either entirely zero or entirely one, and the size of these arrays ought to be obvious from the reference. In order to enhance the link between different regions of images on a global and local scale, the modules work together in a manner that is either multidimensional or multidimensional. By simply including Equation (5b) into the fundamental Karush-Kuhn-Tucker framework, the Inverse Sparse Approximation (ISA) is able to handle a modified Karush-Kuhn-Tucker technique.

$$Xse = \sigma\mu e \qquad (6)$$

Where $\mu = x^{\tau}s/N$ goes to 0 , Whenever it converges, it returns to zero and $\sigma \in [0,1]$is a centeredness element. A σ closer to 1 will prompt search results further towards the interior $(x, s) > 0$. Moving from a specific point(x, s), The new Karush-Kuhn-Tucker system's orientation might be determined as

$$A^{\tau}A\Delta x - \Delta s = r_d \qquad (7a)$$

$$S\Delta x + X\Delta s = r_e \qquad (7b)$$

The stationary residual r_d and the slackness residual r_e may be expressed as follows:

$$r_d = s - \nabla h(x) \qquad (8a)$$

$$r_e = \sigma\mu e - XSe \qquad (8b)$$

Here,$\nabla h(x) = A^{\tau}Ax - A^{\tau}b + \tau e$ is the gradient of the objective function

$$h(x): \frac{1}{2}\|Ax - b^2\| + \tau e^{\tau}x \qquad (9)$$

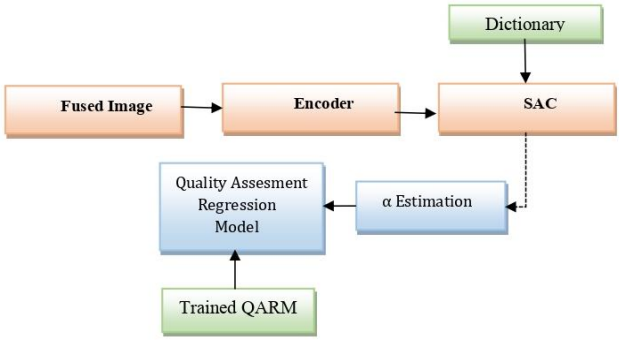

Fig.1. Proposed SAVA based NR-IQ Estimation

An example of Sparse Approximated Code (SAC) with predictor-corrector phases is provided by Algorithm 1, which makes use of the SAC architecture. When compared to the many sparse approximations, it is generally acknowledged to be the most successful candidate. A number of different initializations are used by the SAC that is advised in order to facilitate speedier convergence. These initializations include coefficients that are basic but sufficient, an imaginative pre-conditioner, and adaptive tolerance. During the initial setup and subsequent iterations, the proposed SAC allows for extremely flexible x, s that contradict Equation (5a), despite the fact that Equation (5a) must be met at all times. However, in order for the SAC to be considered adequate, Equation (5a) must first be satisfied by the process of convergence.

The SAC network takes encoded feature vectors as input and uses them as $X = [x_1, x_2, \dots x_k]$ Where k stands for the amount of encoded coefficients used in each computation. An approach suggested for hastening the framework's convergence, Min-Max Normalization gradually transforms and normalizes the variables for every data dimension to the [0,1] range.

$x = [\frac{x-min}{max-min}]$ A minimum and maximum value are included in every column. Each column also has a minimum value. Convolution is performed once data restructuring is finished by converting the 1 by 1024 deep characteristics to a $32x2$ matrix.

The following outcome is seen when thej^{th} feature map is applied to the i^{th} unit of the l convolution layer:

$$x_i^{l,j} = \sigma[b_j + \sum_{a=1}^{m} w_a^j \, x_{i+a-1}^{l-1,j}] \qquad (10)$$

The activation function is denoted by σ, the weight of the j^{th}feature map and a^{th} filter index is denoted as w_a^j, m is the kernel size, and b_j is the bias term for the j^{th} feature map.

B) Modified Level Set And Markov Random Field (MLs-MRF) IQA:

FCM, which stands for fuzzy C-mean, is a fuzzy clustering approach that is often used for the purpose of medical picture segmentation [17]. The FCM algorithm is responsible for dividing the sequence $\{x_k\}_{k=1}^{\mathcal{N}}$ into clusters by striving to minimize the objective function that is provided.

$$\mathcal{J} = \sum_{i=1}^{c} \sum_{k=1}^{\mathcal{N}} u_{ik}^{m} \|x_k - v_i\|^2 \qquad [11]$$

x_k = Gray Value associated with k^{th} pixel

v_i = i^{th}Cluster Center

u_{ik} = Fuzzy menmbership Value of pixel k

m = Fuzziness Exponent with valuelarger than 1

Following these steps, the results of the fuzzy clustering are used to initialize the level-set function.

$$\mathcal{M}_{i,j} = \text{Membership Function}$$

$$\mathcal{Z}_{i,j} = \text{ROI extracted fromImage}$$

A ROI is computed using,

$$\mathcal{Z}_{i,j} = \begin{cases} 1, & u_{ij} > b_0 \\ 0, & otherwise \end{cases}$$

$$b_0 \in (0,1)\ is \text{ adjustable threshold}$$

The level-set function is set up initially as:

$$\varphi_0(x, y) = 2\varepsilon\left(2\mathcal{Z}_{i,j} - 1\right)$$

$$\varepsilon = \text{ constant meant for regularizing the Dirac function}$$

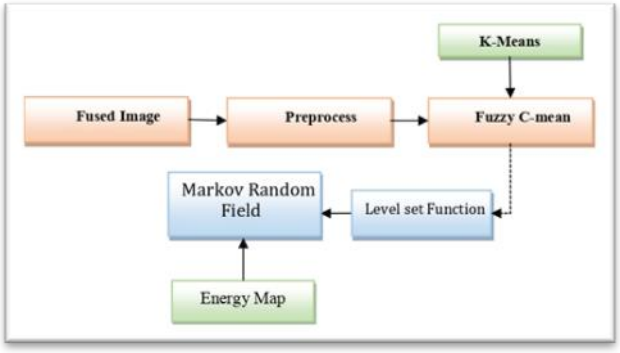

Fig.2. Proposed Modified Level Set And Markov Random Field based NR-IQ Estimation

Controlling parameters are manually input in traditional levelset approaches, and the values of these parameters change depending on the application. This is done in order to influence the progression of the level-set function on the level. The technique that has been described makes use of the outputs of fuzzy segmentation in order to carry out an incremental evaluation of all controlling parameters. To determine the area and length of a contour that was created by fuzzy clustering, the Heaviside and Dirac functions are used in the calculation process.

$$\mathcal{C}_{\text{Area}}(\varphi \geq 0) = \int_{-\Omega}^{\Omega} \mathcal{H}\left(\varphi(x, y)\right) dx\, dy \qquad [12]$$

$$\mathcal{C}_{\text{Length}}(\varphi = 0) = \int_{-\Omega}^{\Omega} \delta_0\left(\varphi(x, y)\right) |\nabla\varphi(x, y)| dx\, dy \qquad [13]$$

It is possible to express the Heaviside function in this context as follows:

$$\mathcal{H}(\varphi) = \begin{cases} 1, & if\ \varphi \geq 0 \\ 0, & if\ \varphi < 0 \end{cases} \qquad [14]$$

An efficient representation of the local interactions between the characteristics of neighboring pixels may be achieved via the use of the Markov Random Field (MRF), which is a complicated stochastic modelling tool. This can be accomplished by using the MRF. There is a random field that can be seen inside the area of hierarchical random field models.

$$a = (a_1, \dots, a_{\mathcal{N}})$$

$$a_i = \text{Feature Value of Pixel}$$

Which attempts to derive an underlying stochastic field.

$$\text{Hidden Random Field} = (\mathscr{b}_1, \dots, \mathscr{b}_{\mathcal{N}})$$

$$\mathscr{b}_i \in \mathcal{K}$$

$$\mathcal{K} = \text{set of all possible labels.}$$

$$\mathscr{b}_i = \text{configuration of labels}$$

If the Markovian requirement that is shown below is satisfied, then the label field a_i should be considered an MRF in regard to its neighborhood system.

$$\rho(a|\mathscr{b}) = \prod_{i \in \mathcal{S}} \rho(a_i|\mathscr{b}_i) \qquad [15]$$

$$\mathcal{S}\ Spot\ related\ to\ another\ one\ another\ with$$

$$neighbourhood\ System$$

$$\mathcal{N} = \{\mathcal{N}_i, i \in \mathcal{S}\}$$

$$\mathcal{N}_i = \text{ pots adjacent to pixel } i$$

$$\mathscr{b}_{\mathcal{N}i} = \text{Neighbourhood Configuration}$$

The equation z_1 of MRF, which describes conditional independence, seems to be as follows:

$$\rho(a|\mathscr{b}) = \rho(a|\mathscr{b})\rho(x) = \rho(\mathscr{b}) \prod_{i \in \mathcal{S}} \rho(a_i|\mathscr{b}_i) \qquad [16]$$

$$\rho(a_i, \mathscr{b}_i|\mathscr{b}_{\mathcal{N}i}) = \rho(a_i|\mathscr{b}_i)\rho(\mathscr{b}_i|\mathscr{b}_{\mathcal{N}i}) \qquad [17]$$

Assuming a is selected at random from a probability distribution $f(a; \mathscr{k}, \theta)$, for $\mathscr{k} \in \mathcal{K}$, the marginal probability of a_i is given by:

$$\rho(a_i|\mathscr{b}_{\mathcal{N}i}, \theta) = \sum_{\mathscr{k} \in \mathcal{K}} \rho(a_i, \mathscr{k}|\mathscr{b}_{\mathcal{N}i}, \theta) = f(a_i, \theta_{\mathscr{k}})\, \rho(\mathscr{k}|\mathscr{b}_{\mathcal{N}i}) \qquad [18]$$

Measurement of the HMRF using the EM algorithm:

$$\widehat{\mathscr{b}} = \arg\max_{\mathscr{b}} \{\rho(a|\mathscr{b}, \Theta)\rho(\mathscr{b})\} \qquad [19]$$

A Gibbs distribution may be thought of as an alternative way to describe an MRF:

$$\rho(\mathcal{b}) = z^{-1} exp\left(-\mathcal{V}_{(\mathcal{b})}\right) \quad [20]$$

$$z: \text{normalization constant}$$

$$\mathcal{V}_{(\mathcal{b})} = \text{potential function}$$

In Equation [12], the prior probability $\rho(\mathcal{b})$ is a Gibbs distribution, and its joint probability is expressed as

$$\rho(a|\mathcal{b}, \Theta) = \prod_i \rho(a_i|\mathcal{b}, \Theta) = \prod_i \rho(a_i|\mathcal{b}_i, \theta_{\mathcal{b}i}) \quad [21]$$

$$\rho(a_i|\mathcal{b}_i, \theta_{\mathcal{b}i}): \text{Gaussian distribution with parameters}$$

$$\theta_{\mathcal{b}i} = (\mu_{\mathcal{b}i}, \Sigma_{\mathcal{b}i})$$

Experiments

Numerous pieces of information pertaining to photo databases are included in Table 1. The RIN represents the number of reference photographs, the DIN represents the number of images that have been warped, and the DTN represents the number of different forms of distortion. The specific score type (SST) is a subjective score. SR stands for the subjective score range category.

The first database comprises one hundred photographs that have been purposefully distorted, with a total of three different types of distortion. There were a total of fifteen observers who were responsible for assigning the DMOS values to the database, which ranged from 0 to 1. The DMOS value and the image quality are said to have a negative relationship with one another.

The second database, which consisted of a distorted photo dataset marked with blur, was examined by around 10 different observers independently. It comes with 250 pictures that include genuine blur distortions, such as blur caused by motion and blur caused by ordinary out-of-focus blur.

Database 3 is comprised of one hundred photographs that have been purposefully altered and twisted according to two distinct methods. The database was evaluated by twenty observers from three different countries using a MOS scale that ranged from 0 to 9. If the MOS score was greater, it suggested that the image quality was better.

Table:1 Database

	RIN	DIN	DTN	SST	SSR
Database 1	25	20	3	DMOS	[0,1]
Database 2	20	200	1	MOS	[0,9]
Database 3	25	80	2	MOS	[0,5]

To measure the accuracy and reliability of the predictions, we used both PLCC and Spearman's rank order correlation coefficient (SRCC). In order to determine the SRCC, you must:

$$\text{SRCC} = 1 - \frac{6\sum_{i=1}^{N} di^2}{N(N^2-1)'} \qquad [21]$$

The variation in the ranks of the i^{th} picture in the objective and subjective evaluations is denoted by di, and N is the quantity of photos in the testing database. The following formula is used by the PLCC to find out how closely the expected scores match the actual facts:

$$\text{PLCC} = \frac{\sum_i (q_i-\bar{q})(s_i-\bar{s})}{\sqrt{\sum_i (q_i-\bar{q})^2}\sqrt{\sum_i (s_i-\bar{s})^2}'} \qquad [22]$$

The objective score of the i^{th} image after nonlinear regression is represented by q_i, and their mean value is $\bar{q}$. In this context, s_i is the subjective evaluation of the i^{th} picture and $\bar{s}$ is the average of the overall s_i. If both indices are rising, it means the quality metric is succeeding.

Performance Evaluation:

In the next part, we will analyses the performance of the two suggested methods on the datasets that were taken into consideration while determining the degree of blur and distortion. Five cutting-edge BIQA algorithms were utilized by the researchers to conduct the same test and analyses the levels of performance that each algorithm exhibited. HyperNet [5], DBCNN [6], CaHDC [7], UNIQUE [8], CLRIQA [9], and VCRNet [10] are some examples of quality evaluations that are based on deep learning [28]. A representation of the experimental findings from the synthetic picture database may be seen in Figure 3.

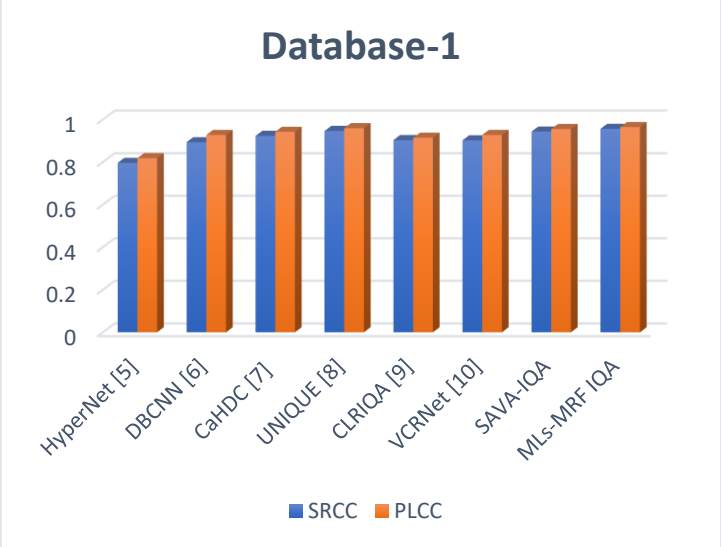

Fig-3 Comparison of State of the art method SRCC & PLCC for database-1

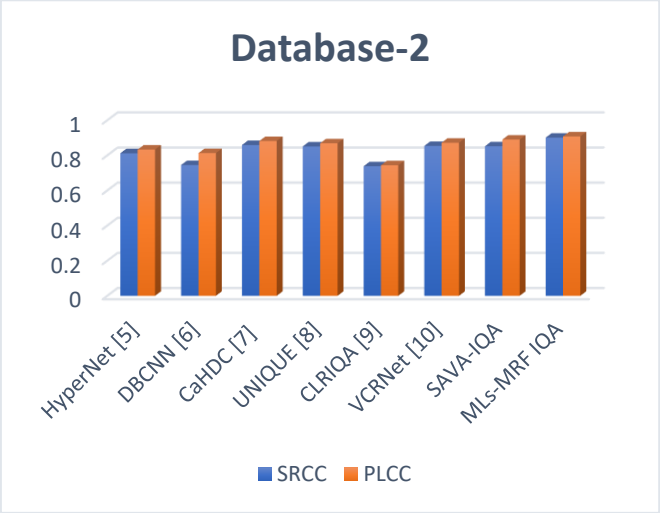

Fig-4 Comparison of State of the art method SRCC & PLCC for database-2

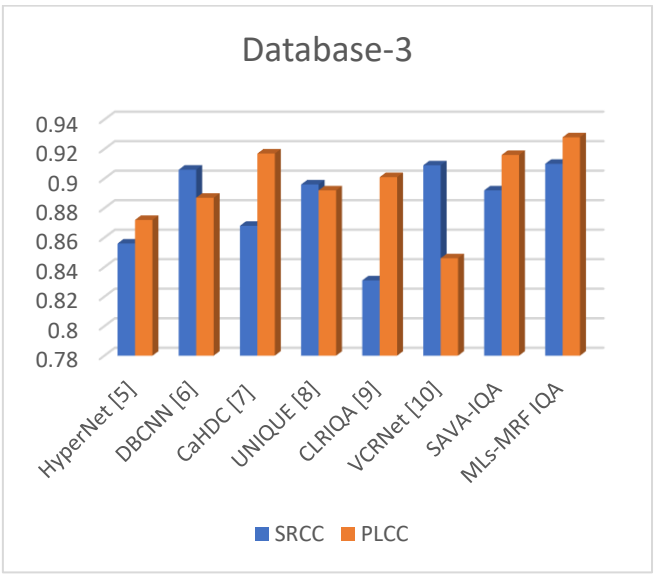

Fig-5 Comparison of State of the art method SRCC & PLCC for database-3

It can be seen from the table that both approaches resulted in promising results. The algorithm that was proposed to be used in dataset 1 received SRCC and PLCC scores of 0.96 and 0.96, respectively, making it the approach that performed the best overall. In addition, SAVA-IQA accomplished a satisfactory level of performance, achieving scores of 0.94 and 0.95 for SRCC and PLCC, respectively. Based on the information provided in the section on linked work, they have a tough time dealing with complicated distortion and blur. It was shown in the earlier research and conclusions that the MLs-MRF IQA technique performed more effectively. This result was achieved by the use of Level Set and Markov Random Field, in addition to the method that was utilized to simulate the human visual system.

Conclusion:

The evaluation of picture quality without reference is an important area of research in the field

of computer vision that has garnered a significant amount of research attention from academics. There have been considerable contributions made by the scientific community to the development of models that function exceptionally well. One of the novel approaches that we proposed for assessing the quality of photographs is one that does not need reference photographs. Compared to other methods, our satellite image statistics-based technique is superior when it comes to evaluating the quality of photos that do not have any references. The purpose of this research is to provide two different NR-IQA techniques. The first one is a combination of Quality Assessment Regression and a Sparse Approximated Code-based Variational Autoencoder. In this method, distortions are evaluated by extracting quality-aware features from the spatial domain as well as the spatial-temporal domain. In addition to this, an objective quality measure is developed by the use of a Markov random field. Additionally, our model consistently offers cutting-edge performance across a wide range of datasets, which is a significant advantage.

Conflicts of Interest

The authors declare that they have no known competing financial interests or personal relationships that could have appeared to influence the work reported in this paper

References

[1] J. Jia et al., “Tradeoffs in the spatial and spectral resolution of airborne hyperspectral imaging systems: A crop identification case study,” IEEE Trans. Geosci. Remote Sens., vol. 60, pp. 1–18, 2022. Art. no. 5510918.

[2] Xu, Shaoping & Jiang, Shunliang & Min, Weidong. (2016). No-reference/Blind Image Quality Assessment: A Survey. IETE Technical Review. 34. 1-23. 10.1080/02564602.2016.1151385.3]

[3] S. Athar and Z. Wang, “A comprehensive performance evaluation of image quality assessment algorithms,” IEEE Access, vol. 7, pp. 140030–140070, 2019.

[4] Hu, L.; Peng, J.; Zhao, T.; Yu, W.; Hu, B. A Blind Image Quality Index for Synthetic and Authentic Distortions with Hierarchical Feature Fusion. Appl. Sci. 2023, 13, 3591. https://doi.org/10.3390/app13063591

[5] S. Bosse, D. Maniry, K. -R. Müller, T. Wiegand and W. Samek, "Deep Neural Networks for No-Reference and Full-Reference Image Quality Assessment," in IEEE Transactions on Image Processing, vol. 27, no. 1, pp. 206-219, Jan. 2018, doi: 10.1109/TIP.2017.2760518.

[6] W. Zhang, K. Ma, J. Yan, D. Deng and Z. Wang, "Blind Image Quality Assessment Using a Deep Bilinear Convolutional Neural Network," in IEEE Transactions on Circuits and Systems for Video Technology, vol. 30, no. 1, pp. 36-47, Jan. 2020, doi: 10.1109/TCSVT.2018.2886771.

[7] J. Wu, J. Ma, F. Liang, W. Dong, G. Shi and W. Lin, "End-to-End Blind Image Quality Prediction With Cascaded Deep Neural Network," in IEEE Transactions on Image Processing, vol. 29, pp. 7414-7426, 2020, doi: 10.1109/TIP.2020.3002478.

[8] W. Zhang, K. Ma, G. Zhai and X. Yang, "Uncertainty-Aware Blind Image Quality Assessment in the Laboratory and Wild," in IEEE Transactions on Image Processing, vol. 30, pp. 3474-3486, 2021, doi: 10.1109/TIP.2021.3061932.

[9] OU, F-Z, WANG, Y-G, LI, J, ZHU, G & KWONG, S 2022, 'A novel rank learning based no-reference image quality assessment method', IEEE Transactions on Multimedia, vol. 24, pp. 4197-4211. https://doi.org/10.1109/TMM.2021.3114551

[10] Pan Z, Yuan F, Lei J, Fang Y, Shao X, Kwong S. VCRNet: Visual Compensation Restoration Network for No-Reference Image Quality Assessment. IEEE Trans Image Process. 2022;31:1613-1627. doi:

10.1109/TIP.2022.3144892. Epub 2022 Feb 1. PMID: 35081029.

[11] Liu C., et al. No-reference image quality assessment of multi-level residual feature augmentation. SIViP (2022). https://doi.org/10.1007/s11760-022-02335-8

[12] N. Badal, et.al. "No Reference Pansharpened Image Quality Assessment Through Deep Feature Similarity," in IEEE Journal of Selected Topics in Applied Earth Observations and Remote Sensing, vol. 15, pp. 7235-7247, 2022, doi: 10.1109/JSTARS.2022.3199446.

[13] Z. Zhou, F. Zhou and G. Qiu, "Blind Image Quality Assessment based on Separate Representations and Adaptive Interaction of Content and Distortion," in IEEE Transactions on Circuits and Systems for Video Technology, doi: 10.1109/TCSVT.2023.3299328.

[14] Sheng Yang, Qiuping Jiang, Weisi Lin, and Yongtao Wang.: An end-to-end saliency-guided deep neural network for no-reference image quality assessment. In Proc. of ACM MM, 2019.

[15] Varga, D. No-Reference Image Quality Assessment with Convolutional Neural Networks and Decision Fusion. Appl. Sci. 2022, 12, 101. https://doi.org/10.3390/app12010101

[16] Lu, Y.et.al.," Blind image quality assessment based on the multiscale and dual-domains features fusion". In Concurrency and Computation: Practice and Experience; Wiley: Hoboken, NJ, USA, 2021; p. e6177.

[17] N.R. Pal, K. Pal, and J. C. Bezdek, "A mixed c-means clustering model," in IEEE Int. Conf. Fuzzy Systems, Spain, 1997, pp. 11–21

[18] R. Ferzli and L.J. Karam. A no-reference objective image sharpness metric based on the notion of just noticeable blur (JNB). IEEE Transactions on Image Processing, 18(4):717–728, 2009.

[19] N.D. Narvekar and L.J. Karam. A no-reference perceptual image sharpness metric based on a cumulative probability of blur detection. In International Workshop on Quality of Multimedia Experience, pages 87–91, 2009.

[20] S. Suthaharan. No-reference visually significant blocking artifact metric for natural scene images. Journal of Signal Processing, 89(8):1647 – 1652, 2009.

[21] S. Varadarajan and L.J. Karam. An improved perception-based no-reference objective image sharpness metric using iterative edge refinement. In International Conference on Image Processing, pages 401–404, 2008.

[22] Mittal, A., A. K. Moorthy, and A. C. Bovik. "No-Reference Image Quality Assessment in the Spatial Domain." IEEE Transactions on Image Processing. Vol. 21, Number 12, December 2012, pp. 4695–4708.

[23] Mittal, A., A. K. Moorthy, and A. C. Bovik. "Referenceless Image Spatial Quality Evaluation Engine." Presentation at the 45th Asilomar Conference on Signals, Systems and Computers, Pacific Grove, CA, November 2011.

[24] N. Venkatanath, D. Praneeth, Bh. M. Chandrasekhar, S. S. Channappayya, and S. S. Medasani. "Blind Image Quality Evaluation Using Perception Based Features", In Proceedings of the 21st National Conference on Communications (NCC). Piscataway, NJ: IEEE, 2015.

[25] Sheikh, H. R., Z. Wang, L. Cormack and A.C. Bovik, "LIVE Image Quality Assessment Database Release 2 ", https://live.ece.utexas.edu/research/quality/.

[26] Mittal, A., R. Soundararajan, and A. C. Bovik. "Making a Completely Blind Image Quality Analyzer." IEEE Signal Processing Letters. Vol. 22, Number 3, March 2013, pp. 209–212.

[27] Patil, M. S., & Mane, P. B. . (2024). No Reference Quality Assessment Metric for Multi-spectral and Multi-Modal Image Fusion using Sparse Approximate Variational Autoencoder. International Journal of Intelligent Systems and Applications in Engineering, 12(17s), 724–732.

[28] M. S. Patil and P. B. Mane, "Fused Image Classification using Pre-trained Deep Convolutional Neural Networks," 2023 Third International Conference on Artificial Intelligence and Smart Energy (ICAIS), Coimbatore, India, 2023, pp. 1215-1221, doi: 10.1109/ICAIS56108.2023.10073743.